J Mol Model (2014) 20:2481
DOI 10.1007/s00894-014-2481-4

ORIGINAL PAPER

Size dependent structural, electronic, and magnetic properties of Sc_N (N=2-14) clusters investigated by density functional theory

Snehasis Bhunia · Nidhi Vyas · Chandan Sahu · Animesh K. Ojha

Received: 1 May 2014 / Accepted: 28 September 2014 / Published online: 22 October 2014

Abstract Structural, electronic, and magnetic properties of Sc_N (N=2-14) clusters have been investigated using density functional theory (DFT) calculations. Different spin states isomer for each cluster size has been optimized with symmetry relaxation. The structural stability, dissociation energy, binding energy, spin stability, vertical ionization energy, electron affinity, chemical hardness, and size dependent magnetic moment per atom are calculated for the energetically most stable spin isomer for each size. The structural stability for a specific size cluster has been explained in terms of atomic shell closing effect, close packed symmetric structure, and chemical bonding. Spin stability of each cluster size is determined by calculating the value of spin gaps. The maximum value for second-order energy difference is observed for the clusters of size N=2, 6, 11, and 13, which implies that these clusters are relatively more stable. The magnetic moment per atom corresponding to lowest energy structure has also been calculated. The magnetic moment per atom corresponding to lowest energy structures has been calculated. The calculated values of magnetic moment per atom vary in an oscillatory fashion with cluster size. The calculated results are compared with the available experimental data.

Keywords Cluster physics · DFT · Magnetic moment · ?Size dependent properties

Electronic supplementary material The online version of this article (doi:10.1007/s00894-014-2481-4) contains supplementary material, which is available to authorized users.

S. Bhunia · A. K. Ojha (✉)
Department of Physics, Motilal Nehru National Institute of Technology, Allahabad 211004, India
e-mail: animesh198@gmail.com

A. K. Ojha
e-mail: animesh@mnnit.ac.in

N. Vyas
Department of Chemistry, Indian Institute of Technology Bombay, Powai 400076, India

C. Sahu
Department of Spectroscopy, Indian Association for the Cultivation of Science, Jadavpur, Kolkata 700032, India

Introduction

For the last two decades, a variety of theoretical and experimental studies have been done to identify the size dependent structural, electronic, optical, and magnetic properties of atomic clusters [1–6]. These properties are neither similar to those observed at atomic scale nor at the bulk form. It is expected that materials assembled from finite-sized clusters may have special properties. Also, these properties are changed drastically with the change of cluster size [1–13], and it can be investigated by employing the cluster dynamics approach. The cluster dynamics (CD) is based on kinetic equations describing the formation and evolution of clusters. The magnetic behavior of clusters with different geometry is investigated by DFT within the quantum Heisenberg model. Magnetic property of the clusters depends on the valence electron of the cluster, symmetry, geometry, and size. The valence electrons mediate the exchange interaction between neighboring magnetic moment localized on the core electrons of the atoms. It is to be believed that anomalous behavior of magnetism in low-dimensional transition metals can be attributed to the enhancement of densities of d states at the Fermi level resulting from spatial confinement [14]. The shifting of 3d electrons is sensitive to changes in the positions of the atoms which is responsible for the change in magnetic

moment with change of cluster size. The symmetry of cluster is another important issue which can contribute to the change in magnetic property. It is because of the fact that symmetry enables degeneracy and magnetism originates due to degeneracy [15]. Therefore, an enhancement of the magnetic moment is to be expected as long as the cluster possesses geometry of high symmetry with lowest structural energy, which is a challenging task for the theoreticians. The magnetic property of the cluster also depends on the optimization at different spin states. The calculation at different spin states causes change in spin density localized at the atoms, which ultimately change the magnetic moment of the cluster.

The structural and magnetic properties of the transition metal clusters have been a subject of intense research for theoretical and experimental scientists owing to enhanced magnetic properties for the smaller size cluster compared to its bulk counterparts [6–13]. The study on emergence of magnetic properties from atoms to the bulk form is the important aspect which provides the idea to develop magnetic nanomaterial [7] and tractable models for the better understanding of the effect of spin coupling in finite and low dimensional systems. The transition metals have already been taken into account by the theoretical scientists for exploring size dependent magnetic properties due to partly filled 'd' shell ($3d^n4s^2$, n=1-9) which results in a number of spin isomers within a very close energy range [6–16]. Within this close energy, the structure of each spin isomer of Sc_N clusters has different structural, electronic, and magnetic properties. The magnetic moment of the transition metals is dominated by the spin contribution from the highly localized 3d electrons, and therefore these metals are a good example of localized ferro magnets. The 3d electron shell can accommodate ten electrons, and according to the Hund's rule a half filled shell has five electrons with parallel spin. It is important to note that the system such as transition and rare earth metals, the behavior of the valence electrons is crucial since these electrons mediate the exchange interaction between neighboring magnetic moments localized on the parent atoms. The electron configuration of an isolated Sc is [Ar] $3d^14s^2$. The magnetism in Sc clusters is obviously governed by the unpaired valence electron, in contrast to the local magnetic moment observed in the clusters of heavy rare earth elements due to the presence of the inner electron. Due to enhanced magnetic properties of Sc at low dimensional range, it may be used in the device application such as bio-sensing. To the best of our knowledge, few theoretical studies have been done on magnetic properties of Sc_N clusters as a function of cluster size [17–20]. Recently, the magnetic properties of Sc_N clusters of various size (N=5–20) have been investigated through Stern-Gerlach molecular-beam deflection experiment [7]. The results of the experiment confirm that all Sc_N clusters are elemental molecular magnets with a strong magnetic moment for Sc_{13} cluster. In a theoretical study [20], the authors have reported the size dependence on structural, electronic, and magnetic properties of Sc_N clusters of different sizes using DFT. They have performed all calculations on clusters by considering symmetric structure, as the initial guess, and the results thus obtained were used to calculate the magnetic properties. They also have reported that the most stable cluster of each size may be obtained only by performing the symmetry based restricted calculations.

In the present work, we have explored the role of asymmetric structural calculations (without putting symmetry as constraints while optimizing the structure of Sc_N clusters) on structural and magnetic properties of Sc_N clusters of different size. Further, we have also compared the calculated results of asymmetric calculations with those done for symmetric calculations for the same cluster size. The reason behind performing the present study is based on the fact that in the case of asymmetric calculation, the most stable structure of Sc_N clusters may have structural energy far away from the value of structural energy calculated through symmetric calculation. Thus, there is a possibility that the stability of different spin isomer might also be changed. According to the Jahn-Teller theorem [21], every nonlinear molecule or crystal that has orbital electronic degeneracy is unstable when the nuclei are in a symmetrical configuration with respect to at least one asymmetric distortion of the nuclei, which lifts the degeneracy. In this work, we focus on the size dependence of structural stability, spin stability, HOMO-LUMO gap, electron affinity, vertical ionization energy, chemical hardness, and magnetic moment of Sc_N clusters. Further, we have also studied the variation in Raman features of Sc_5 cluster of various spin states. The authors do believe that the present report will shed light on how these properties vary for Sc_N (N=2-14) clusters with size.

Computational procedure

All the calculations have been carried out using DFT. Depending on the reliability of DFT [16] studies on the choice of functional and the basis set for the purpose under investigation, the DFT calculations are done by treating the exchange-correlation interaction by expanding the electron orbital size, not the shape. The standard LANL2DZ basis set of primitive Gaussians have been used to expand the cluster orbitals formed by the $3d^14s^2$. The remaining 28 core electrons, $1s^2\ 2s^2\ 2p^6\ 3s^2\ 3p^6$ of the Sc atom are represented by the Wadt-Hay effective core potential [22]. In the present study, all geometry optimizations are carried out with the DFT method based on the gradient-corrected exchange-correlation functional of Perdew, Burke, and Ernzerh of PBEPBE [23, 24]. The structures of Sc_N (N=2-14) clusters at different spin states have been optimized using DFT at PBEPBE/LANL2DZ level of

theory. This theoretical method has proven to be a reliable tool for the ab-initio level of study of structure and properties of transition metal clusters [3, 16, 19]. The cluster geometries have been obtained by finding local minima on multi-dimensional potential energy surface. We have applied an efficient scheme of global optimization, called the cluster fusion algorithm [25–27]. It works on the principle based on the partitioning of the data points. In this method, it is assumed that the atoms in a cluster are bound by Lennard-Jones potentials and the growth of cluster takes place by addition of atoms one by one. All atoms of the cluster are allowed to move while the energy of the system is decreased (it happens only when we do not restrict the symmetry of the molecule and allow the program to search the full space of molecular configurational degrees of freedom for getting minima at potential energy surface). The motion of the atoms is stopped when the energy minimum is reached. Otherwise, imposing restriction, the optimization process reaches a stationary point (where forces on the atoms are zero) which may be a saddle point. The geometries and energies of all cluster isomers are calculated without imposing any symmetry restriction. The most stable cluster configuration (lowest energy isomer) is then used as the starting configuration for the next step of the cluster growing process. The optimization of cluster structure at the minimum of the potential energy surface is confirmed by the calculation of vibrational frequencies. The absence of imaginary frequency corresponding to each geometry of Sc_N clusters confirms that the optimization has been done at the minimum of the potential energy surface.

All the calculations have been performed using GAUSSIAN 09 software package [28]. The existence of a large number of energetically close lying different spin states causes the calculation of ground state structure difficult for the theoretical scientists. In order to find most stable structures, the geometries are optimized without giving any symmetry based constraints. We have computed the effect of spin multiplicity on the structure and energy of Sc_N (N=2-14) clusters by varying its value from 1 to 7.

Results and discussion

Optimized structure of different spin isomers of Sc_N (N=2-14)

The size dependent investigation of different properties of transition metals in various spin states is still a challenge for both experimentalists and theoreticians. Although, few experimental and theoretical studies on Sc_N clusters of various size have been done [17–20], however their results are not consistent with each other.

The most stable structure of Sc_N (N=2-14) clusters for each cluster size has been presented in Fig. 1. Our calculation shows that the most stable structure of Sc_2 cluster to be singlet. The singlet state structure is energetically more favorable over the second most stable structure at quintet state by 0.02 eV. This value is much closer to the value of energy difference Sc_2 cluster between singlet and quintet spin states of Sc_2 cluster reported in the earlier study [20]. In the present report, the computed dissociation energy of Sc_2 cluster is 1.68 eV. It is in good agreement with the experimentally measured value of 1.65±0.22 eV [7]. The average value of bond length turns out to be 2.30 Å. This value slightly under estimates the bond distance reported in an earlier study [20]. The dissociation energy of Sc_2 cluster in quintet spin state is calculated to be 1.67 eV, which is also in good agreement with the experimentally observed value [29]. We have also performed several energetically close-lying spin isomers of Sc_2. After singlet and quintet spin states structure of Sc_2, the next most stable spin state structure is triplet having dissociation energy 1.56 eV, which is 0.12 eV lower than that of dissociation energy of quintet state. The order of stability of Sc_2 cluster is calculated to be singlet>quintet>triplet>nonet>septet. For the Sc_3 cluster, the lowest energy spin isomer is found to be doublet having isosceles triangle type of structure with an angle 57.73^0 and dissociation energy 2.48 eV. The average bond length between the Sc atoms is calculated to be 2.776 Å. The second energetically most stable spin state structure of Sc_3 is octet, which have nearly isosceles triangle type structure with angle 63.34^0. The values of dissociation energy and average bond length for this spin state structure are calculated to be 2.16 eV and 2.86 Å, respectively. The quartet spin state structure of Sc_3 is the third most stable structure having dissociation energy 0.35 eV higher than that of the doublet spin state. In this spin state the Sc_3 cluster also maintained its isosceles triangular structure. Sextet spin state structure of Sc_3 cluster is nearly an isosceles triangle having dissociation energy lower than that of the values of other spin states isomers. Although, the structures of low-lying spin isomers of Sc_3 cluster are not much different from each other except the value of average bond length. It has been observed that the value of average bond length is increased when we move away from the most stable spin isomer.

For optimizing the Sc_N structure of different spin isomers of a particular size cluster, the same initial guess has been given to obtain the lowest energy state structure. As a result, the structure of some low-lying spin isomers for each cluster size appears differently than that of the structure reported in an earlier study [20]. The most stable spin isomer for Sc_4 is found to be triplet state, which is a tetrahedron with D_{2d} symmetry. The nearest low-lying spin isomer of Sc_4 is found to be singlet state having $C_{2\nu}$ symmetry with structural energy 0.24 eV greater than that of the most stable structure [20]. The order of structural stability of different spin isomers of Sc_4 is found to be in the order of triplet>singlet>quintet. In the case of Sc_5, the energetically most favorable spin state structure is doublet having bi-pyramid structure with C_1 point group symmetry.

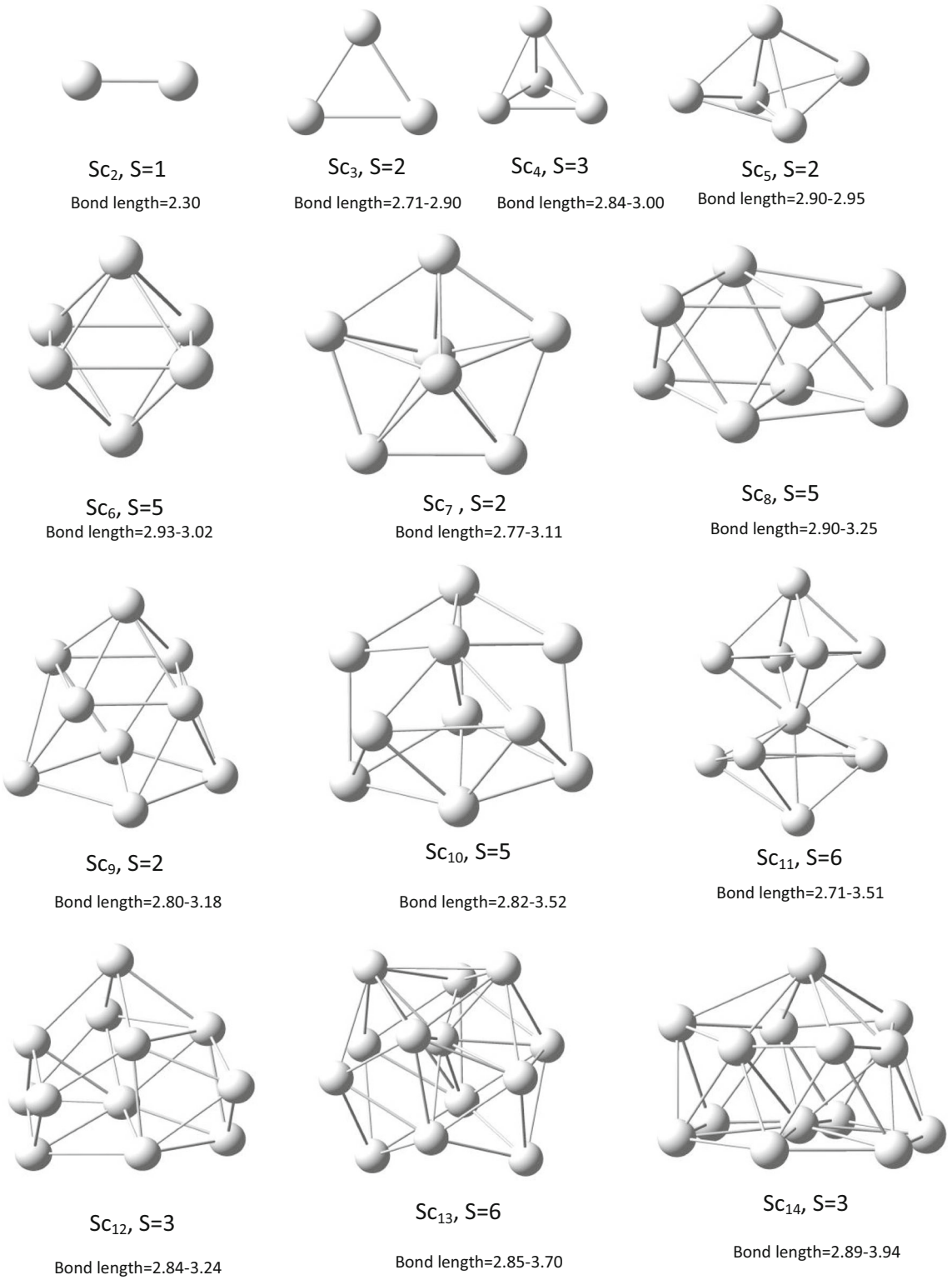

Fig. 1 Most stable geometries of Sc_N (N=2-14) clusters. The value of bond length has been presented in range (min-max)

The first low lying spin isomer near to doublet spin state is quartet having energy 0.01 eV higher than that of the energy of the most stable spin state isomer. The order of structural stability for Sc_5 is found to be in the order of doublet>quartet>sextet>octet. The most stable isomer for Sc_6 is octahedron with quintet spin state and having $C_{2\nu}$ symmetry. The next stable structure of Sc_6 is triplet state having octahedron configuration with C_{2h} symmetry and its

structural energy is 0.10 eV greater than that of the most stable structure. After quintet and triplet, another low lying structure of Sc_6 is singlet spin state with D_{2h} symmetry. The structural energy of singlet spin state structure is 0.39 eV higher than that of quintet state. The most stable geometry of different spin isomers of Sc_7 cluster turns out to be pentagonal bi-pyramid. However, the structural symmetry of some spin isomers is found to be different. The doublet state with C_{2V} symmetry is found to be more stable than that of octet and sextet spin state structure by 0.08 and 0.09 eV, respectively. It is interesting to note that the octet (C_{5h}) and sextet (C_{2V}) states are energetically degenerate states since the energy difference between these two spin isomers is only 0.007 eV. These degenerate spin isomers have not been reported previously [20]. For $Sc_{8,}$ the quintet state structure turns out to be bi-capped octahedrons with C_2v structural symmetry. It is energetically found to be more stable than that of other spin states structure, singlet and triplet. Similar types of structure have been found for singlet and triplet states having C_s symmetry. The structural energy of singlet and triplet spin sates is greater by 0.09 eV and 0.44 eV, respectively than that of the energy of quintet spin state.

For Sc_9, the lowest energy structure is found to be single capped tetragonal prism structure in a doublet spin state. A similar single capped tetragonal prism type structure in quartet state is also found which is energetically quasi-degenerate with the doublet spin state structure by 0.04 eV. Further, single capped tetragonal structure has been obtained for the sextet spin state whose structural energy is 0.05 eV larger than that of doublet spin state isomer. For Sc_{10}, the minimum energy spin isomer is calculated to be quintet state and the next minimum energy conformer is found to be singlet state with the energy difference of 0.0008 eV. The difference in structural energy is very tiny and therefore these two spin state structures are said to be degenerate with C_1 point group symmetry. Minimum low energy structure of Sc_{11} is a distorted D_{4d} structure in sextet spin state. A similar type of structure is also found in quartet spin state at energy 0.02 eV higher than the sextet spin state structure. The triplet spin state structure of Sc_{12} is found to be energetically more stable than that of singlet and quintet spin state structures. The triplet spin state structure is more stable by 0.12 eV and 0.31 eV, respectively compared to singlet and quintet spin state structures. For Sc_{13}, the lowest energy structure is found to be sextet with distorted I_h symmetry. The quartet spin state structure is found to be the second most energetically stable structure having energy higher by 0.007 eV than that of the sextet spin state. Here, these two structures exist in degenerate state. A triplet spin state isomer with nearly spherical compact C_s symmetry structure is found to be energetically the most stable for Sc_{14}. The order of structural stability is found to be in the order of triplet>quintet>singlet. The value of average bond length corresponding to the most stable spin isomers for each cluster size is plotted as a function of cluster size and the plotted curve has been shown in Fig. 2. From Fig. 2, it is quite evident that the average bond length for the cluster size (N=2-6) is increased consistently. After the cluster size N=6, the value of average bond length does not show any consistent trend with the cluster size. The change of the average bond length with the cluster size depends on the co-ordination number, compact form, and type of symmetry of the clusters. For the higher value of N, the average bond length approaches the bulk value of the Sc_N clusters [30]. The dissociation energy (D_e) of different spin state isomers of Sc_N (N=2-14) clusters has been calculated using the following equation:

$$D_e(N) = (E_{N-1} + E_1) - E_N. \quad (1)$$

The calculated value of D_e corresponding to each spin isomer of Sc_N (N=2-14) has been presented in Table 1. It is quite evident by looking at the data presented in Table 1 that the most stable spin isomer for each cluster size has the least amount of D_e and its value is decreased consistently according to order of structural stability of the Sc_N (N=2-14) clusters.

Size dependence of average binding energy of Sc_N (N=2-14)

The average binding energy of various spin state isomers of Sc_N (N=2-14) clusters has been calculated by the following expression:

$$E_b/N = E_1 - E_N/N, \quad (2)$$

where E_N is the energy of a neutral N-particle Sc cluster, and E_1 is the energy of a single Sc atom. The calculated value of average binding energy for different spin isomers of Sc_N cluster are presented in Table 1. The calculated value of binding energy per atom corresponding to the most stable spin isomer for each cluster size has been plotted against the cluster

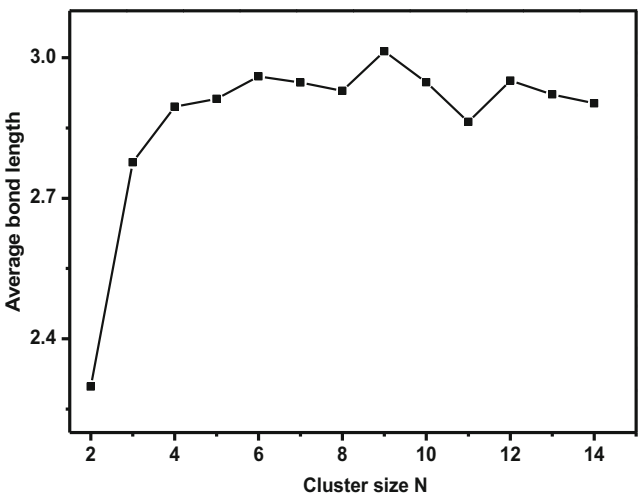

Fig. 2 The variation of average bond length calculated corresponding to the most stable geometry as a function of cluster size (N)

Table 1 The calculated values of binding energy/atom, HOMO-LUMO gap, dissociation energy (D_e), average bond length (d), second order energy difference (Δ_2E) corresponding to most stable structure of Sc_N (N=2-14) clusters

Cluster	Spin multiplicity	Binding energy/atom	HOMO – LUMO (eV)	D_e (N) (eV)	d (Å)	Δ_2E (eV)
Sc_2	singlet	0.84	0.01	1.68	2.30	0.77
	triplet	0.78	0.02	1.56		
	quintet	0.83	0.01	1.66		
	septet	0.55	0.01	1.10		
Sc_3	doublet	1.38	0.02	2.48	2.78	0.03
	quartet	1.26	0.01	2.12		
	sextet	1.23	0.01	2.03		
Sc_4	singlet	1.79	0.03	3.00	2.89	0.20
	triplet	1.85	0.01	3.25		
	quintet	1.75	0.01	2.70		
Sc_5	doublet	2.03	0.01	2.97	2.91	0.02
	quartet	2.07	0.01	2.96		
	sextet	2.09	0.01	3.04		
	octet	2.04	0.02	2.80		
Sc_6	singlet	2.19	0.01	2.69	2.96	0.35
	triplet	2.23	0.01	2.97		
	quintet	2.23	0.02	3.07		
Sc_7	doublet	2.42	0.01	3.43	2.95	0.02
	quartet	2.40	0.20	3.30		
	sextet	2.41	0.01	3.35		
Sc_8	singlet	2.42	0.01	2.44	2.93	0.13
	triplet	2.47	0.01	2.79		
	quintet	2.48	0.01	2.88		
Sc_9	doublet	2.54	0.01	3.01	3.01	0.05
	quartet	2.53	0.01	2.97		
	sextet	2.53	0.01	2.96		
Sc_{10}	singlet	2.58	0.002	2.96	2.95	0.52
	triplet	2.59	0.003	3.13		
	quintet	2.58	0.01	2.96		
Sc_{11}	quartet	2.56	0.04	2.42	2.86	1.09
	sextet	2.57	0.04	2.42		
Sc_{12}	singlet	2.64	0.005	3.40	2.95	0.02
	triplet	2.65	0.01	3.53		
	quintet	2.62	0.04	3.21		
Sc_{13}	doublet	2.67	0.04	2.91	2.92	0.99
	quartet	2.68	0.04	3.05		
	sextet	2.68	0.04	3.06		
Sc_{14}	singlet	2.76	0.001	3.83	2.90	
	triplet	2.78	0.01	4.05		
	quintet	2.77	0.008	4.01		

size in Fig. 3. For small Sc_N clusters, N=2-6 the binding energy per atom increases steadily with the cluster size and upon further increasing the cluster size from N=7-14, the binding energy per atom increases almost linearly. The maximum value of binding energy per atom for N=13 and 14 indicate the high stability of Sc_N clusters. The average binding energy of Sc_{14} is 2.78 eV. This value is enhanced with increasing the cluster size and therefore it may gradually approach to the value corresponding to bulk form, 3.9 eV [30]. The value of binding energy corresponding to different spin state isomers for each cluster size has been plotted against the cluster size, N and it has been shown in Fig. 4. The difference in binding energy between the most stable spin state and the second most stable spin isomer lies in the energy range 0.02–0.07 eV for all cluster size. It suggests that the ensemble of energetically low-lying isomers would be thermally available at relatively low temperature circumstances [16].

In order to have more insight about the cluster stability, the analysis of the second order difference of the binding energy for energetically most stable cluster has also been calculated

for each cluster size. In cluster physics, the second-order difference (Δ_2E_n) of the cluster energy is defined as:

$$\Delta_2 E_N = E_{N+1} + E_{N-1} - 2E_N, \quad (3)$$

where E_N, E_{N+1}, and E_{N-1} are the cluster energy of size N=N, N+1, and N-1, respectively. The plot between second order energy difference and cluster size has been shown in Fig. 5. From Fig. 5 one can easily notice that the prominent maxima occurs at N=2, 11, 13. It implies that these sizes of the clusters are highly more stable than that of their neighboring size. The other local peaks are found for N=6 and 10 clusters. The enhanced cluster stability for a specific size cluster can be explained in terms of three factors, atomic shells closing effects, close packing symmetric structure [20], and chemical bonding [1]. The valence electronic configuration of Sc is $3d^14s^2$ and the total number of the valence electrons in Sc_2, Sc_6, and Sc_{11} clusters are 6, 18, and 33, respectively. The number of electrons in these three clusters is consistent with the closure of electronic shell within the elliptical spherical Jellium model [31]. Therefore these clusters may have additional structural stability as we have observed in the form of maximum value of Δ_2E_n. Moreover, the total number of the valence electrons of cluster Sc_{10} is 30, which is approximately close to applicability of closure of electronic shells within the elliptical spherical Jellium model. Therefore, the special stability for a specific size (N=2, 6, 10, and 11) clusters may be the result of coexistence of atomic motif and electronic ordering, which play an important role in determining the stability of these clusters. Indeed, the enhanced stability of Sc_6, Sc_{11}, and Sc_{13} clusters arises when their ionic structure is highly symmetric and corresponds to the icosahedral type of packing [16]. This icosahedral growth sequence for metal clusters has also been seen for clusters of alkaline earth metals such as Sr [32] and Ba [33], which exhibit non-metal to metal transitions with increasing cluster size. It is important to note that for alkaline earth metal clusters there is a strong competition between atomic and electronic shells closure [32, 34]. On the other hand, the chemical bonding could also be responsible for the better stability of specific size cluster [35]. Depending on the structural geometry, the increase in coordination number and decrease of interatomic distance could also enhance the binding energy of Sc_N clusters. These factors improve the delocalization of 3d electrons, which causes the reduction of local magnetic moment of Sc_N cluster [34]. Contrary to it, the E_b could also be enhanced by increasing the exchange splitting of 3d orbit, which would further increase the magnetic moment. The competition between these two governs the resultant stability of Sc_N clusters [35].

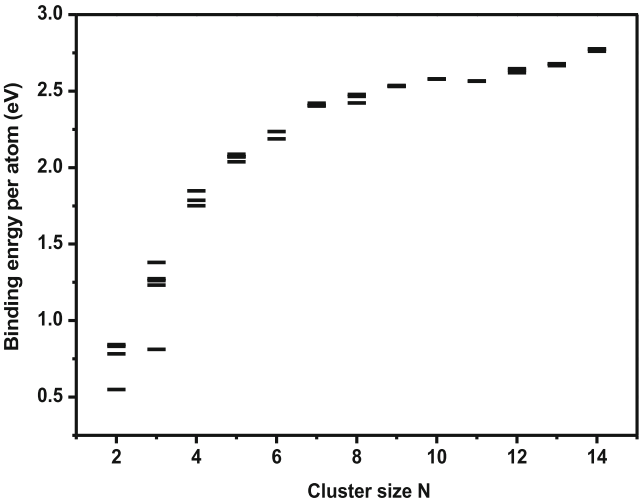

Fig. 4 Binding energy calculated for each spin isomer of Sc_N (N=2-14) cluster as a function of cluster size (N)

Size dependence of HOMO-LUMO gap of Sc_N (N=2-14)

The HOMO-LUMO gap of the transition metal cluster is an important qualitative characteristic to study the modification

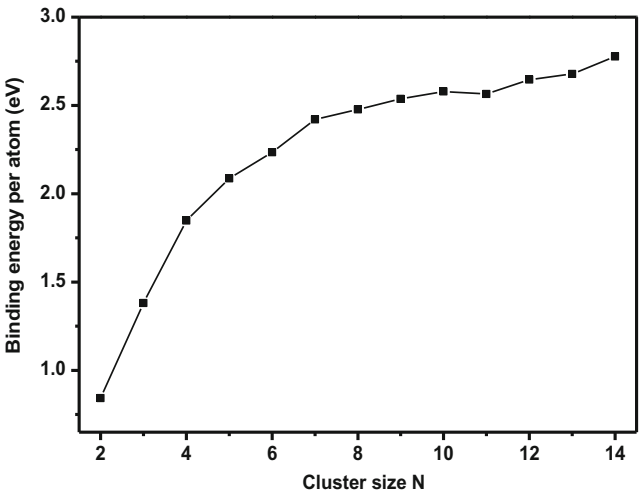

Fig. 3 Binding energy per atom calculated corresponding to the most stable geometry as a function of cluster size (N)

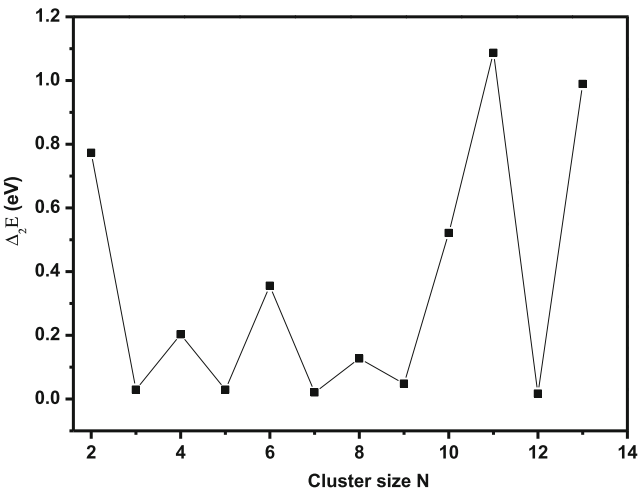

Fig. 5 Second order energy difference Δ_2E calculated corresponding to the most stable geometry of Sc_N (N=2-14) cluster as a function of cluster size (N)

in band structure with size of cluster. The HOMO-LUMO gap is also used to determine the ability of a molecule or cluster to participate in the chemical reactions. The value of HOMO-LUMO gap has been calculated for each spin isomer for all cluster sizes and the value thus obtained by the calculation has been plotted as a function of cluster size, N. The variation of HOMO-LUMO gap with the cluster size is shown in Fig. 6. From Fig. 6, one can easily notice that the value of HOMO-LUMO gap changes abruptly with cluster size, even with the different spin isomers of the same cluster size. From Fig. 6, it is quite clear that the prominent peak occurs magically at N=7, 11, and 13 indicating the extra high chemical stability for Sc_7, Sc_{11}, and Sc_{13} clusters. Here, we would like to mention that the stability of Sc_7 cluster is also consistent with the electron shell model. Although, the shell model neglects the core potential of the atoms in the clusters however it uses the Jellium model, which considers the positive charges of the atoms being smeared out to a homogeneous background. However, for metal clusters with highly delocalized valence electrons, the electronic-shell model can be applied [31].

Sc is a transition metal atom which includes both localized 3d electrons and delocalized 4s electrons. These electronic (3d, 4s) states have different cluster size dependence. Sc has double s electron outside a closed shell. The energy of 3d state lies just below the energy of 4s state, which is expected to influence the cluster properties. The metal clusters with closed electron shells are spherical but with increasing the cluster size toward the bulk Sc, the clusters with open electronic shells are deformed from the spherical shape. The deformation in the shape causes changes to the electron-shell energies. In case of spin isomers of the same cluster size, the shape is deformed due to the Jahn–Teller effect and due to the change in shape the electron shell energy could also be changed and therefore contribution of 3d state to the density of states at the Fermi level might be changed. The 4s state are delocalized and confined by the boundaries of the cluster and relevantly show strong discontinuous size dependent variations. Due to the above facts, the HOMO-LUMO gap changes abruptly with varying the cluster size and different spin isomer of same cluster size. The changes in the value of HOMO-LUMO gap for Sc_N (N=2-14) clusters and its different spin isomers indicate the alternation of metal and non-metal like behavior.

Spin-stability of Sc_N (N=2-14)

The spin gaps (δ_1, δ_2) are another qualitative feature of the metal cluster to determine the size dependent spin stability of the cluster and it is defined as [20]:

$$\delta_1 = -\left[\varepsilon_{HOMO}^{majority} - \varepsilon_{LUMO}^{minority}\right],$$
$$\delta_2 = -\left[\varepsilon_{HOMO}^{minority} - \varepsilon_{LUMO}^{majority}\right].$$

In general, the spin isomer of a particular size cluster is said to be magnetically stable if the values of δ_1 and δ_2 are positive. The magnetic stability exits when the LUMO of the majority manifolds (spin-up) lies above the HOMO of the minority (spin-down) manifolds and vice versa. The values of δ_1, δ_2 and Eg (HOMO-LUMO gap) have been calculated for the most stable cluster of each size and the calculated values are plotted against the cluster size, N and presented in Fig. 7. From Fig. 7, one can easily notice that the values of both, δ_1 and δ_2 are positive for the Sc_N (N=2-14) cluster. Thus, the Sc_N clusters reported in the present study are found to be magnetically stable. Further, it has also been observed by looking at Fig. 7 that the values of δ_1 and δ_2 are decreased consistently with increase of cluster size from N=3 to N=10. However, two local prominent maxima occurs at N=11 and N=13, which correspond to the high magnetic stability of Sc_{11} and Sc_{13} clusters.

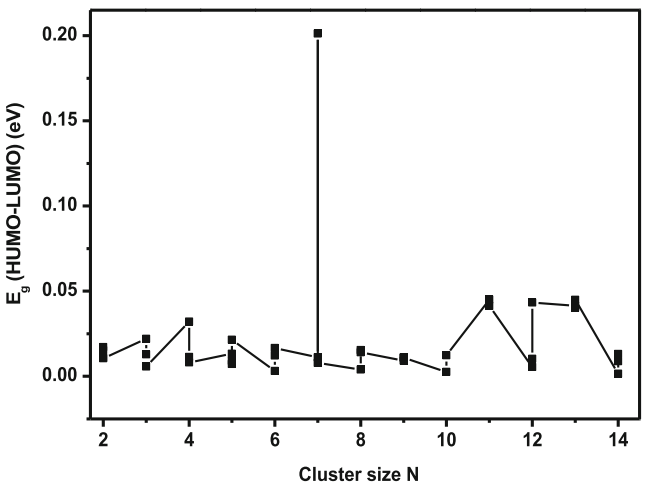

Fig. 6 The HOMO-LUMO (E_g) calculated for each spin isomers of Sc_N (N=2-14) as a function of cluster size (N)

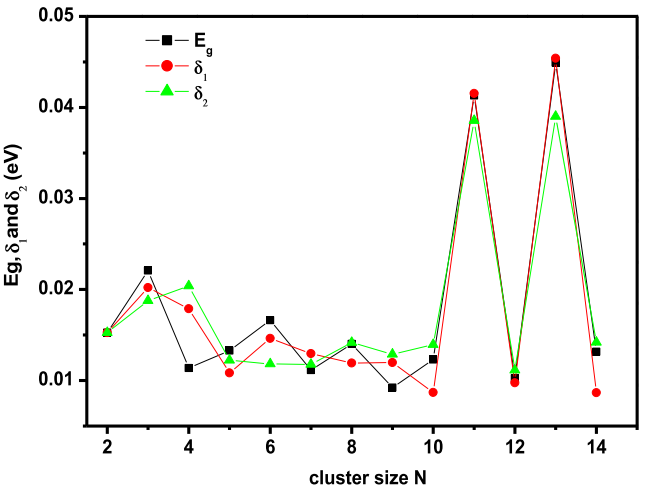

Fig. 7 The HOMO-LUMO (E_g), spin stabilities (δ_1 and δ_2) calculated corresponding to the most stable geometry of Sc_N (N=2-14) as a function of cluster size

Vertical ionization energy and electron affinity of Sc_N (N=2-14)

The most familiar theoretical method used to evaluate the ionization energy (IE) and electron affinity (EA) of atomic cluster is IE=E (Sc_N^+) – E (Sc_N) and EA=E (Sc_N) – E (Sc_N^-) where E (Sc_N^+), E (Sc_N^-), and E (Sc_N) are the total energies of the cation, anion, and neutral clusters, respectively. The values of E (Sc_N^+) and E(Sc_N^-) are calculated at the optimized geometries of neutral clusters. The above total energy based on vertical method provides comparatively better results. However, in this method, the possible error occurs in total energy values due to the approximations used in the theoretical models. Since the values of ionization energy and electron affinity are highly sensitive to the incorporation of electron correlation in the calculation method they demand the use of a relatively larger basis set [36, 37]. Thus in order to minimize this error, we have performed all the calculations using the larger basis set, LANL2DZ. The IE and EA can also be calculated using Koopmans' theorem. However, we have not used this method for calculating IE and EA since it considers the relaxation of the spin orbitals (spin orbitals in the N-1 electron states are identical with those of the N-electron state) which tend to produce too positive ionization potential and too negative electron affinity [32]. The values of IE and EA for the most stable cluster of each size have been plotted as the function of cluster size, N and it is shown in Figs. 8 and 9, respectively. From Fig. 8, it is clear that the ionization energy decreases gradually with increasing the cluster size and an opposite trend has been observed for the variation of electron affinity with cluster size (see Fig. 9). At larger cluster size, the values of IE and EA vary asymptotically. The asymptotic behavior of IE and EA can be explained by the semi classical theory derived by Smith [38] and Wood [39]. They proposed the

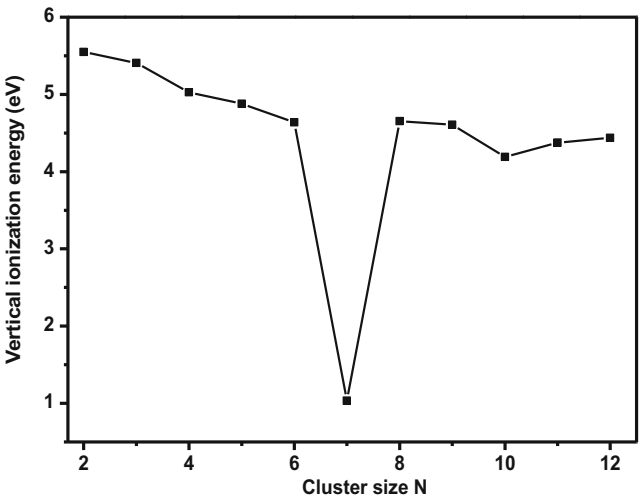

Fig. 8 Vertical ionization energy calculated corresponding to the most stable geometry of Sc_N (N=2-14) cluster as a function of cluster size (N)

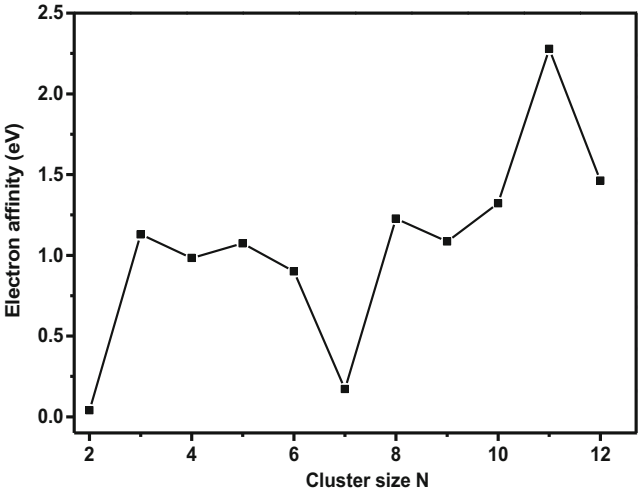

Fig. 9 Electron affinity calculated corresponding to the most stable geometry of Sc_N (N=2-14) cluster as a function of cluster size (N)

following relationships for determination of IE and EA for a metal sphere with radius R and work function W:

$$\mathrm{IE} = \mathrm{W} + \frac{3}{8}\frac{1}{R} \tag{4}$$

$$\mathrm{EA} = \mathrm{W} - \frac{5}{8}\frac{1}{Rs}. \tag{5}$$

Further, the asymptotic behavior of IE and EA can also be explained by the quantum based theory [1]. Since the excess charge in a metal at equilibrium is located on the surface, the change of surface and curvature energies with cluster size affects the ionization energy and electron affinity of the clusters. A large dip at N=7 in IE for Sc_7 cluster may be explained in terms of close-shell electronic configuration of the Sc_7^+ (outer total free electron 20) cluster.

Chemical hardness of Sc_N (N=2-14)

We use the Koopmans's formula to calculate the chemical hardness of the Sc_N (N=2-14) clusters. It provides sufficiently good results [40–42] due to the omission of electron correlation which tends to cancel the aforementioned relaxation error. According to the Koopmans's formula, the chemical hardness is defined as [38]:

$$\eta \approx \frac{1}{2}\ (\varepsilon_{LUMO} - \varepsilon_{HOMO}). \tag{6}$$

Figure 10 represents the chemical hardness of Sc_N cluster as a function of the cluster size, N. The value of η for Sc_3 and Sc_{13} cluster is calculated to be 0.275 and 0.481 eV, respectively. Thus, the Sc_{13} is the most stable cluster followed by Sc_3. In fact, chemical hardness depends on the ionization energy. The ionization potential of small cluster having s

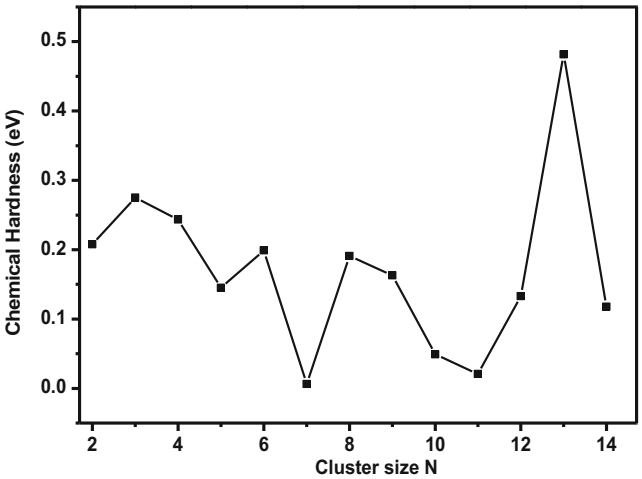

Fig. 10 Chemical hardness calculated corresponding to the most stable geometry of Sc_N (N=2-14) cluster as a function of cluster size (N)

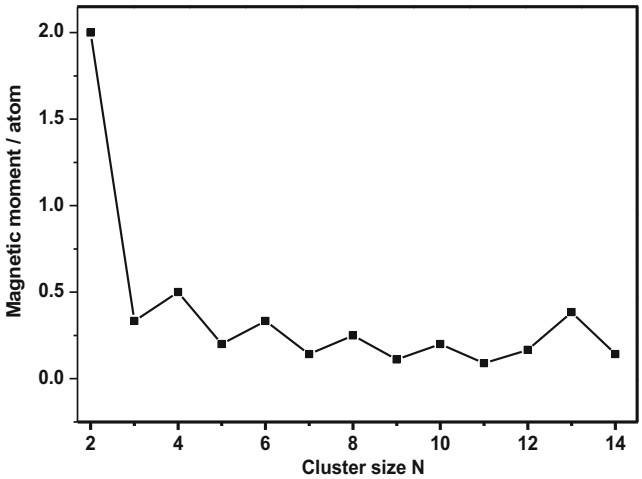

Fig. 11 The value of magnetic moment per atom calculated corresponding to the most stable geometry of Sc_N (N=2-14) cluster as a function of cluster size (N)

electron in its outer most shell shows an even odd alternation. The even size clusters systematically have slightly larger (0.1-0.5 eV) ionization potential than that of the odd size clusters. The odd-even alternation also appears in the mass abundance spectra [41]. This odd-even effect is observed up to some limiting cluster size, which depends on the particular element. The odd-even effects can be explained in terms of stabilization of cluster due to electron pairing effect of s electron [43].

Size dependence of magnetic properties of Sc_N (N=2-14)

The magnetism of small size clusters depends on symmetry of the cluster, atomic coordination, and interatomic distances between neighbor atoms [16]. According to Hund's rule the electronic configurations of Sc is $3d^1\uparrow 4S^2$. Sc atom has one un-paired spin, which may be responsible for its magnetic behavior. When atoms condense to form a cluster or a metal, the overlap between the atomic orbitals of neighboring atoms leads to the formation of bands of electronic levels. The orbitals corresponding to 4s electrons produce a nearly free electron band, whereas the d electrons stay localized on the atomic sites having band width value in the range 5–10 eV [1]. The crystal potential stabilizes the d and s states by different magnitudes. This process and partial hybridization between the s and d shells leads to charge transfer from s to d states. In order to investigate the size dependent magnetic properties of Sc_N (N=2-14) clusters, the structure of Sc_N clusters are optimized without putting the symmetric restriction. The magnetic moment per atom for the structurally most stable spin isomer of each size of Sc_N (N=2-14) clusters is plotted as a function of cluster size, N and presented in Fig. 11. The magnetic value of magnetic moment per atom calculated corresponding to the most stable spin isomer along with the experimental value [7] of magnetic moment per atom is given in Table 2. From Fig. 11, one can easily notice that the even size cluster possess greater magnetic moment than that of the odd size cluster. As expected, the value of magnetic moment is larger for the cluster of smaller size (N=2-4), which has also been observed in an earlier study [20]. The value of magnetic moment of the cluster for N=2, 3, and 4 is calculated to be 2.0, 0.33, and 0.50 μ_B, respectively. The magnetic moment has been calculated for the cluster size (N=2-4) is in good agreement with the values reported in an earlier study [20]. The value of magnetic moment calculated for each cluster size decays separately for even and odd number of clusters, which also supports the odd-even effect in the clusters up to cluster size N=12. In the case of cluster size (N>6), the local maxima of the magnetic moment occurs at (N=13) and the value is calculated to be 0.38 μ_B. It is in good agreement with the value observed experimentally [7]. From the experimental values presented in Table 2, one can easily notice that the greater magnetic moment of the Sc_N cluster is obtained for N=13 within the range of cluster size (N=5-18). The calculated values of

Table 2 The total magnetic moment (μ) and magnetic moment (μ)/atom corresponding to the most stable structure of Sc_N (N=2-14) cluster

N	$\mu(\mu_B)$	μ/atom(μ_B)	Exp. (ref. 7) (μ_B)
Sc5	1	0.200	0.170±0.017
Sc6	2	0.333	0.218±0.011
Sc7	1	0.143	0.131±0.008
Sc8	2	0.250	0.246±0.009
Sc9	1	0.111	0.112±0.005
Sc10	2	0.20	0.154±0.140
Sc11	3	0.27	0.140±0.010
Sc12	2	0.167	0.187±0.007
Sc13	5	0.386	0.461±0.017
Sc14	2	0.14	0.126±0.007

magnetic moment corresponding to the most stable Sc_N clusters match nicely with the experimentally observed values (see Table 2). The deviation between the computational and experimental values of magnetic moments for cluster size N=6, 10, and 13 turn out to be less than 0.02 μ_B/per atom.

In order to demonstrate the variation of magnetic ordering (ferromagnetic and ferrimagnetic) with the cluster size, we have performed the Mulliken analysis for atomic spin density of Sc_N clusters. In the present study, size dependent ferromagnetic and ferrimagnetic ordering are observed in the Sc_N clusters. The ferromagnetic ordering of spin (aligned parallel order) of Sc_N clusters has been obtained for cluster size N≤6. The ferrimagnetic ordering of the spins is observed for Sc_7 cluster where one spin has a value of 0.77 μ_B and is aligned antiparallel to the other remaining spins. In the case of Sc_8, the three spins are aligned antiparallel to the other reaming spins. Thus, the competition of spin alignment between parallel and antiparallel spins is continued for the clusters of other sizes also. For Sc_{13}, there are two anti-parallel spins one due to core atom and another one due to surface atom. For Sc_{14}, there are also two anti-parallel spins, existing on the closely placed side to side of the surface atoms. Except for the cluster of smaller size, the larger value of magnetic moment per atom is observed for the Sc_{13} cluster and found to have ferrimagnetic ordering.

In an earlier study [20], "effective" magnetic moment of each size cluster has been calculated from spin-weighted averages over the quasi-degenerate structures using the following the relationship:

$$\overline{S} = \frac{\sum_i (2S_i + 1)S_i}{\sum_i (2S_i + 1)}, \tag{7}$$

where, S_i is the total magnetic moment of the corresponding ith isomer of the corresponding cluster structure. The value of average spin magnetic moment of different spin isomers of Sc_N cluster (N=2-14) has been calculated using the above equation. The value of the effective magnetic moment calculated from spin-weighted averages is not well supported by the values [7]. The measured value of magnetic moment of Sc_N (N=2-18) clusters was reported to lie in between the values of magnetic moment of the most stable spin isomer and the second most stable spin isomer [1]. For example, the calculated value of magnetic moment of Sc_{11} for the most stable spin isomer (doublet) is 0.091 μ_B/atom and the magnetic moment of second most stable spin isomer (quartet) is 0.273 μ_B/ atom. The experimental value of magnetic moment per atom for this cluster size is reported to be 0.140±0.010 μ_B/atom. It is quite evident that the experimental value of magnetic moment is lying in between the theoretically calculated value of magnetic moment corresponding to the most stable and the second most stable spin isomers. A similar trend has also been observed in our present study. Since, the experimental value of magnetic moment lies in between the value of magnetic moments of the most stable and the second most stable spin isomers, it is therefore not possible to consider the cluster of fractional multiplicity for performing the theoretical calculations. Here, we would only calculate the average magnetic moment per atom corresponding to the lowest energy spin isomers of Sc_N (N=2-14) clusters theoretically and compared these values with the experimental results. Another reason for this discrepancy could be due to the fact that the energetically close spin isomers cannot be nicely distinguished in Stern-Gerlach deflection experiments [2] because of the limited resolving ability of the experimental apparatus. Further, DFT computed structures in their static states (0 K) whereas the experimental data is measured at finite temperature (58±2 K) [2]. Further, for computing the magnetic property of the cluster by DFT calculation, two issues (i) a possible non-collinear (NC) setting of magnetic moments (i.e., a smooth variation of magnetic density vector from point to point in space), and (ii) spin-orbit interaction (SOI) must be taken into account. However, difficulties in combining NC spin density with the IOC and choice of correct non collinear solution among many metastable configurations may also be responsible for departure of calculated values of magnetic moment of the cluster from the experimentally observed value. The change of temperature may cause structural changes such as; structural energy and structural symmetry for different spin isomers clusters. As a result, the multiplicity of the most stable spin isomers may also change by changing the temperature. The variation of temperature (low to high or high to low) causes transition of spin states for the different spin isomer structures. However, an earlier study [44], reported that the spin can couple to the rotation and this combined with spin orbit coupling in Pd atoms provides the mechanism for the transition between the various spin states of Pd clusters. Koster et al. [45] have reported that both bi-layer structures, Cs and C_{3v} of Pd_{13}, are significantly populated in the septet and quintet states even at lower temperature (100 K). However, the lower multiplicities of these two structures are populated at higher temperature. This might be the reason for the reduction of the spin magnetic moment with increasing temperature and causes change in the total magnetic moment of the clusters.

Here, in order to investigate size dependent magnetic moment of Sc_N, we choose the value of the magnetic moment of the most stable structure of Sc_N clusters and plotted the values of magnetic moment as a function of cluster size. The plot is shown in Fig. 11. The magnetic properties of free transition metal clusters have been investigated in the past primarily by means of Stern–Gerlach type experiments [46–50]. Both, the experimental as well as theoretical results (see Fig. 11) have shown a strong enhancement of the magnetic moment per atom for smaller size clusters. By the increase of cluster size, the magnetic moment per atom slowly approaches to the bulk value in an oscillatory fashion. Another interesting point of

this result is that the magnetic moment decays separately for even and odd number of cluster size, which also supports the odd-even effect in the clusters. The decay of magnetic moment with the increase of cluster size can be explained by considering the Friedel model [51] and using the Jensen and Bennemann [52] equation for magnetic moment. The average magnetic moment depends on sensitively the ratio between the number of surface atoms and the bulk-like atoms.

$$\mu_i = \left(\frac{z_b}{z_i}\right)^{1/2} \mu_b \, if \, Z_i \geq Z_c, \tag{8}$$

where Z_i ,Z_b are the local atomic co-ordination number and bulk atomic co-ordination number, respectively. Z_c is a threshold value of atomic coordination number below it, local magnetic moment of that atom adopts the value μ_{dim} of the dimer. Surface atoms have small values of Z_i and large values of μ_i, whereas the internal atoms have $Z_i=Z_b$ and $\mu_i=\mu_b$. Most atoms of the small clusters are on the surface and hence the value of $\overline{\mu}$ is large. On increasing the cluster size, the fraction of surface atoms decreases and the value of $\overline{\mu}$ also decreases. Considering magnetic moments μ_s for the surface atoms and μ_b for the bulk atoms, Jensen and Bennemann [52] calculated the average magnetic moment of the cluster using the following equation: [46]

$$\overline{\mu} = \mu_b + (\mu_s - \mu_b) N^{-\frac{1}{3}}, \tag{9}$$

where N is the number of atoms in the corresponding clusters. This formula also indicates a smooth decrease of $\overline{\mu}$ toward the bulk magnetic moment with increasing cluster size.

Raman spectra of different spin isomers of Sc_5

In order to correlate the structural stability with spectroscopic properties of different spin isomers for a particular size of Sc_N clusters, we have simulated the Raman spectra of different spin isomers of Sc_5 cluster. We have chosen Sc_5 for simulating the Raman spectra because of the fact that the structure of different spin isomers of Sc_5 has almost the same symmetry. The simulated spectra of different spin isomers (doublet, quartet, sextet and octet) of Sc_5 cluster are presented in Fig. 12. After optimization, the symmetry of doublet, quartet, and sextet structures of Sc_5 turns out to be C_2 and for octet structure it turns out to be C_{2V}. Although the doublet, sextet, and octet structures belong to the same symmetry, the simulated Raman spectra for these structures appeared differently. Raman spectra of doublet, sextet, and octet spin states structure contain five Raman bands at 110, 132, 162, 194, and 266 cm^{-1}. The intensity of Raman band appearing at 266 cm^{-1} is relatively larger compared to the other four Raman bands. The Raman band at ~266 cm^{-1} is assigned to symmetric ring breathing mode where all the Sc atoms of closed pentagon vibrate coherently. The intensity and position of this band changes with varying the spin state of the structure. However, the Raman features for the quartet structure is entirely different than that of the doublet spin state structure. Further, the Raman spectra of sextet spin state have four Raman bands. The Raman band at ~160 cm^{-1} has larger intensity compared to other Raman bands. Similarly, the Raman spectra of octet spin state have five Raman bands where the band ~158 cm^{-1} has larger intensity. The variation in positions and intensities

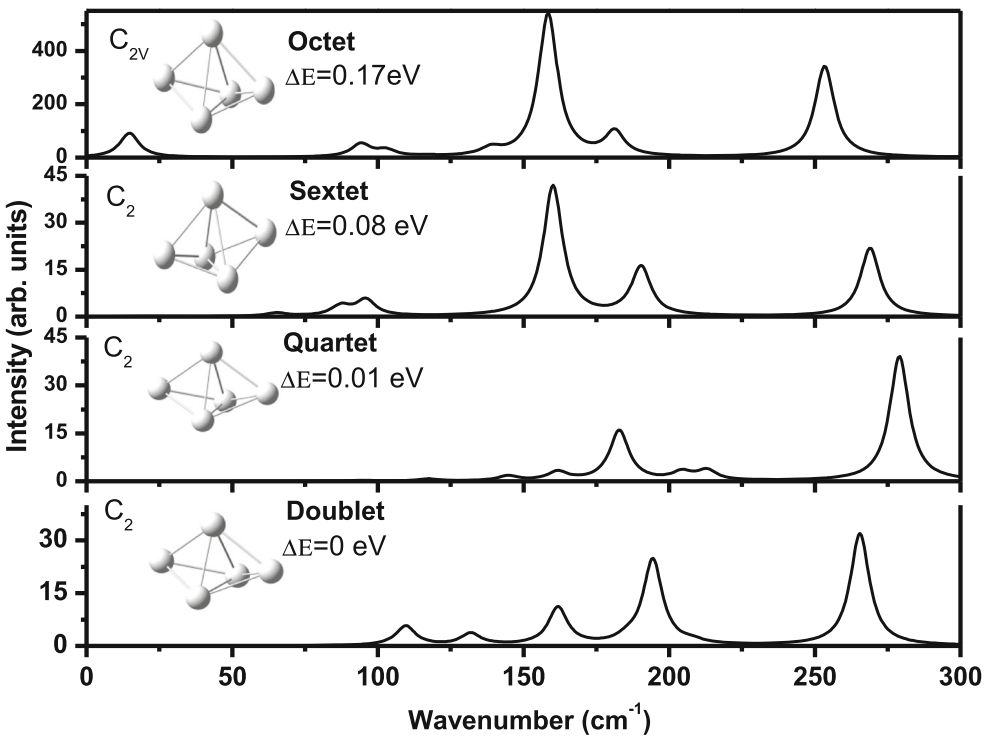

Fig. 12 The calculated Raman spectra of different spin isomers of Sc_5

of Raman bands for different spin states structure of Sc_5 cluster could be due to the overall redistribution of electronic charge density around the cluster, which might be responsible for the change in polarizabilty matrix and consequently change the Raman features of the Sc_5 cluster.

Conclusions

The structural, electronic, and magnetic properties of different spin isomers of Sc_N (N=2-14) clusters have been investigated using DFT at PBEPBE/LANL2DZ level of theory. The greater structural stability of the Sc_N clusters were found for N=2, 6, 10, 11, and 13. On the basis of calculated values of spin gaps energy for each size of cluster, we found that the clusters of size N=11 and 13 are more stable. The present study also provides a comprehensive analysis of variation of vertical ionization energy, electron affinity, and chemical hardness with cluster size. The ionization energy and electron affinity are calculated through the total energy of neutral and ionic states of Sc_N clusters. The values of chemical hardness were calculated using the orbital energies obtained at PBEPBE/LANL2DZ level of theory. The value of magnetic moment per atom calculated corresponding to the energetically most stable Sc_N clusters has shown strong size dependence. The value of magnetic moment/atom is found to be maximum (0.3846 μ_B) for the cluster size, N=13. The value of magnetic moments/atom computed for the most stable spin isomers are in good agreement with the experimentally observed values. Further, a ferromagnetic coupling is found to be energetically more preferred for the clusters of size N≤6 whereas ferrimagnetic coupling is observed for the cluster size, N=7–14. In order to see the changes in the Raman features by varying the spin states of the same size Sc_N cluster, the Raman spectra of different spin states of Sc_5 have also been calculated. A significant change in the Raman features was observed by varying the spin states of the Sc_5 cluster. It could be due to the overall re-distribution of electronic charge density around the cluster, which might be responsible for the change in the polaizability matrix and consequently Raman features appeared differently for the different spin states structure of Sc_5.

Acknowledgments SB and AKO are thankful to the Council of Scientific and Industrial Research (CSIR) for providing financial support through project grant number No. 03(1179)/10/EMR-II. NV would like to acknowledge DST, New Delhi, India for granting Fast-Track Fellowship.

References

1. Alonso JA (2005) Structure and properties of atomic nanoclusters, Chapt 5. Magnetic properties of atomic clusters of the transition elements. Imperial College Press, London, pp 191–210
2. Guet C, Hobza P, Spiegelman F, David D (eds) (2001) Atomic clusters and nanoparticles. NATO Advanced Study Institute, les Houches Session LXXIII, les Houches (2000). EDP Sciences and Springer, Berlin
3. Mei Wang, Xiaowei Haung, Zuliang Du, Yuncai Li (2009) Chem Phys Lett 258–264
4. Reinhard P-G, Suraud E (2004) Introduction to cluster dynamics. Wiley-VCH, Weinheim
5. Baletto F, Ferrando R (2005) Rev Mod Phys 77:371
6. Cramer CJ, Thrular DG (2009) Phys Chem Chem Phys 11:10757
7. Knickelbein MB (2005) Phys Rev B 70:014424
8. Cox AJ, Louderback JG, Bloomfield LA (1993) Phys Rev Lett 71:923
9. Knickelbein MB (2004) Phys Rev B 71:184442
10. Bobadova-Parvanova P, Jackson KA, Srinivas S, Horoi M (2005) J Chem Phys 122:014310
11. Srinivas S, Horoi M, Kohler C, Seifert G (2002) ibid 116:3576
12. Kabir M, Mookerjee A, Kanhere DG (2006) Phys Rev B 73:224439
13. Polesya S, Sipr O, Bornemann S, Minar J, Ebert H (2006) Europhys Lett 74:1074
14. Himpsel FJ, Ortega JE, Mankey GJ, Wills RF (1998) Adv Phys 47:511
15. Dunlap BI (1990) Phys Rev A 41:5691
16. Lyalin A, Solov'yov AV, Greiner W (2006) Phys Rev A 74:043201
17. Wu ZJ, Zhang HJ, Meng J, Dai ZW, Han B, Jin PC (2004) J Chem Phys 121:4699
18. Papai MC (1997) Chem Phys Lett 267:551
19. Papas BN, Schaefer HF III (2005) J Chem Phys 123:074321
20. Wang J (2007) Phys Rev B 75:155422
21. Ham FS (1972) In: Geschwind S (ed) Electron paramagnetic resonance. Plenum, New York, p 1
22. Hay PJ, Wadt WR (1985) J Chem Phys 82:270
23. Perdew JP, Burke K, Ernzerhof M (1996) Phys Rev Lett 77:3865
24. Perdew JP, Burke K, Ernzerhof M (1997) Phys Rev Lett 78:1396
25. Koshelev A, Shutovich A, Solov'yov IA, Solov'yov AV, Greiner W (2003) Phys Rev Lett 90:053401
26. Solov'yov IA, Solov'yov AV, Greiner W (2004) Int J Mod Phys E 13:697
27. Obolensky OI, Solov'yov IA, Solov'yov AV, Greiner W (2005) Comput Lett 1:313
28. Gaussian 09, Revision A.1, Frisch MJ, Trucks GW, Schlegel HB, Scuseria GE, Robb MA, Cheeseman JR, Scalmani G, Barone V, Mennucci B, Petersson GA, Nakatsuji H, Caricato M, Li X, Hratchian HP, Izmaylov AF, Bloino J, Zheng G, Sonnenberg JL, Hada M, Ehara M, Toyota K, Fukuda R, Hasegawa J, Ishida M, Nakajima T, Honda Y, Kitao O, Nakai H, Vreven T, Montgomery JA Jr, Peralta JE, Ogliaro F, Bearpark M, Heyd JJ, Brothers E, Kudin KN, Staroverov VN, Kobayashi R, Normand J, Raghavachari K, Rendell A, Burant JC, Iyengar SS, Tomasi J, Cossi M, Rega N, Millam JM, Klene M, Knox JE, Cross JB, Bakken V, Adamo C, Jaramillo J, Gomperts R, Stratmann RE, Yazyev O, Austin AJ, Cammi R, Pomelli C, Ochterski JW, Martin RL, Morokuma K, Zakrzewski VG, Voth GA, Salvador P, Dannenberg JJ, Dapprich S, Daniels AD, Farkas O, Foresman JB, Ortiz JV, Cioslowski J, Fox DJ (2009) Computational models. Gaussian Inc, Wallingford
29. Akeby H, Pettersson LGM (1993) J Mol Spectrosc 159:17
30. Kittel C (1996) Introduction to solid state physics, 7th edn. Wiley, New York
31. Darke GWF (2006) Atomic, molecular and optical physics. Springer, Berlin
32. Wang Q, Sun Q, Yu J-Z, Gu B-L, Kawazoe Y, Hashi Y (2000) Phys Rev A 62:063203
33. Lyalin A, Solov'yov IA, Solov'yov AV, Greiner W (2003) Phys Rev A 67:063203
34. Lyalin A, Solov'yov AV, Bréchignac C, Greiner W (2005) Phys Rev B 38:L129

35. Fu-Yang T, Qun J, Yuan-Xu W (2008) Phys Rev A 77:013202
36. Simons J, Jordon K (1987) Chem Rev 87:535
37. Shankar R, Senthilkumar K, Kolandaivel P (2009) Int J Quantum Chem 109:764–771
38. Smith JM (1965) J Am Inst Aeronaut Astronaut 3:648
39. Wood MD (1981) Phys Rev Lett 46:749
40. Kolandaivel P, Jayakumar N (2000) Int J Quantum Chem 76:648
41. Padmanabhan J, Parthasarathi R, Subramaniam V, Chattaraj PK (2005) J Phys Chem A 109:11043
42. Senthilkumar K, Kolandaivel P (2002) J Mol Phys 100:3817
43. de Heer WA, Knight WD, Chou MY, Cohen ML (1987) Solid State Phys 40:93
44. Popov AP, Pappas DP, Anisimov AN, Khanna SN (1996) Phys Rev Lett 76:4332–4335
45. Koster AM, Calaminici P, Orgaz E, Roy DR, Reveles JU, Khanna SN (2011) J Am Chem Soc 133:12192
46. Billas IML, Chatelain A, de Heer WD (1994) Science 265:1682
47. Billas IML, Chatelain A, de Heer WD (1997) J Magn Magn Mater 168:64
48. Apsel SE, Emmert JW, Deng J, Bloomfield LA (1996) Phys Rev Lett 76:1441
49. Knickelbein MB (2002) J Chem Phys 116:9703
50. Cox AJ, Lourderback JG, Apsel SE, Bloomfield LA (1994) Phys Rev B 49:12295
51. Friedel J (1969) Transition metals. Electronic structure of the d-band. Its role in the crystalline and magnetic structures. In: Ziman JM (ed) The physics of metals. Cambridge University Press, Cambridge, pp 340–408
52. Jensen P, Bennemann KH (1995) Z Phys D 35:273